Rapid Estimation of the Maximum Communication Distance for an Underwater Laser Communication System

Hu Xiuhan[1,2] Hu Siqi[1,2] Zhou Tianhua[1*] He Yan[1] Zhu Xiaolei[1] Chen Weibiao[1]

[1]*Key Laboratory of Space Laser Communication and Detection Technology, Shanghai Institute of Optics and Fine Mechanics, Chinese Academy of Sciences, Shanghai* 201800, *China*

[2]*University of Chinese Academy of Sciences, Beijing* 100049, *China*

Abstract A semi-analytical method of rapidly estimating the maximum communication distance of an underwater laser communication system is proposed. For a given underwater optical channel, only two simulation times are needed to obtain the maximum communication distance. Once the system conditions are changed, no more simulations are needed. Two reference distances through simple mathematical operations based on the parameters of underwater optical channel are initially deduced. Than a separate simulation is conducted for each reference distance. Finally, an equation for calculating the maximum communication distance is deduced based on theoretical analysis. The simulation results are compared with experimental ones and are found to coincide well with each other. The validation of the semi-analytical method is proved.

Key words optical communications; underwater laser communication; semi- analytical method; maximum communication distance; Monte Carlo method

OCIS codes 060.4510; 010.3310; 010.4450

水下激光通信系统最大通信距离的快速估计

胡秀寒[1,2] 胡思奇[1,2] 周田华[1*] 贺 岩[1] 朱小磊[1] 陈卫标[1]

[1]中国科学院上海光学精密机械研究所空间激光信息传输与探测技术重点实验室, 上海 201800

[2]中国科学院大学, 北京 100049

摘要 为了快速评估水下激光通信系统的最大通信距离,提出了一种半解析的方法。对于给定的水下光学信道,仅仅需要进行两次仿真就可以获得系统的最大通信距离。即使系统参数改变,也不再需要进行额外仿真。根据水下光学信道参数,通过简单的数学运算获得了两个参考距离。并针对每个参考距离各进行了一次仿真。最后根据理论分析和仿真结果,推导出了最大通信距离的计算公式。为了验证该计算方法的有效性,将计算结果与实验结果进行了对比。对比结果表明两者吻合得很好,故所提出的半解析方法的有效性得以证实。

关键词 光通信; 水下激光通信; 半解析方法; 最大通信距离; 蒙特卡罗法

中图分类号 TN929.1 **文献标识码** A

doi: 10.3788/CJL201542.0805007

1 Introduction

Underwater optical communication is attracting increased attention because of its advantages of high speed, good security, and low power consumption[1-3]. Many successful applications have been reported[4-6], but some factors hinder its extensive use, including absorption and scattering of water, energy loss of light, angular diffusion, temporal spreading, and spatial dispersion during underwater propagation. Based on multiple scattering model, Wei

收稿日期: 2015-03-11; **收到修改稿日期**: 2015-04-07

基金项目: 国家863计划(2014AA093301)、国家自然科学基金(61205214)

作者简介: 胡秀寒(1989—),男,博士研究生,主要从事蓝绿激光通信方面的研究。E-mail: huxiuhan@siom.ac.cn

导师简介: 朱小磊(1966—),男,研究员,博士生导师,主要从事全固态激光器技术方面的研究。E-mail: xlzhu@siom.ac.cn

*通信联系人。E-mail: gietzth@163.com

et al. provided a numerical method of determining the time domain dispersion of underwater optical wireless communication[7]. Lerner et al. researched the time- and space-resolved multiple forward scatter of light in natural water by Monte Carlo method[8]. Mullen et al. developed an experimental setup to measure the frequency response of light propagation in Maalox-enhanced water and found that modulation depth remains constant until attenuation lengths (the reciprocal of attenuation coefficient) to about 10[9]. Hanson et al. realized error-free underwater optical communication at 1 Gb/s over a 2 m path in a laboratory water pipe with up to 36 dB of extinction[10]. As we know, the maximum communication distance is an important parameter for an underwater optical communication system, but few related works have been reported. The radiative transfer equation is difficult to directly solve for underwater communication[11-12], so Monte Carlo simulation method is widely used[8-9,13-18]. However, this method is time consuming, and simulation needs to be repeated once system parameters are changed. Indeed, an efficient method of estimating the maximum communication distance is challenging to establish.

Compared with other light sources, a laser is more suitable for long-distance underwater communication. This study focuses on underwater laser communication (ULC) and proposes a semi-analytical method of rapidly estimating the maximum communication distance. With this calculation method, Monte Carlo simulation needs to be conducted only twice for a given underwater optical channel. When system conditions are changed, no more simulation is needed. The method is useful for rapidly estimating the maximum communication distance of a ULC system.

2 Monte Carlo method

2.1 Simulation procedure

Traditionally, Monte Carlo method is based on the brute tracing of photon packets[19-20]. Interactions of laser pulse with water are treated as collisions between photon packets and particles. Fig.1 shows the propagation procedure of a photon packet and the global coordinate $o-xyz$, where L denotes transmission distance. The procedure consists of the following three steps.

2.1.1 Initialization

Initial parameters of a photon packet include initial energy $E_{\mathrm{P\_MC}}$, initial location, initial propagation direction, and launch time. The initial energy of a photon packet is set to

$$E_{\mathrm{P\_MC}} = E_{\mathrm{T\_MC}}/N , \tag{1}$$

where $E_{\mathrm{T\_MC}}$ is the energy of a laser pulse, and N is the number of traced photon packets. Increased N can improve the precision of computation results, but time consumption also increases. Simulation time and statistical accuracy should be simultaneously considered when choosing a suitable N.

2.1.2 Scattering of photon packet

After propagating a random step distance l_{R}, the photon packet arrives at a scattering spot. The random step distance[17] is

$$l_{\mathrm{R}} = -\frac{1}{c}\ln(R_{\mathrm{ud}}) , \tag{2}$$

where R_{ud} is a random value uniformly distributed within 0 to 1, and c is attenuation coefficient. After scattering, the energy of photon packets is adjusted using a single-scattering albedo ϖ, $\varpi = b/(a+b)$ or $\varpi = b/c$, where a and b are absorption and scattering coefficients, respectively. The propagation direction of photon packet also changes after scattering. Here, a local coordinate $o'-x'y'z'$ is built, where o' is scattering spot and z' is the propagation direction of photon packet before scattering. The scattering direction is determined by the azimuth angle φ and the scattering angle θ. The azimuth angle φ is uniformly distributed within 0 to 2π [21]. The polar angle θ is also defined as scattering angle. The distribution function of scattering angle is governed by a scattering phase function. The Henyey - Greenstein function is convenient for code development and debugging and is thus frequently used as

phase function[22]:

$$P(\theta)=\frac{(1-g^2)}{2\pi(1-2g\cos\theta+g^2)^{3/2}}, \tag{3}$$

where g is the average value of $\cos\theta$, named as asymmetry factor. The new propagation direction after scattering should be converted from local coordinate to global coordinate before sampling a new random step distance.

2.1.3 Receiving judgment

The propagation-scattering procedure is repeated when one of the following two events occurs. Firstly, if the energy of photon packet is too small and negligible, the photon packet is considered as absorbed. The photon packet survival threshold is set to $10^{-10}E_{\mathrm{P\_MC}}$ to balance both simulation time and statistical accuracy[21]. Secondly, if the photon packet's propagation path intersects the receiver plane within the receiver aperture and field of view (FOV), it is marked as effectively received. When the tracing procedure of all photon packets is complete, we use the statistical properties of all received photon packets to represent the properties of received laser pulse.

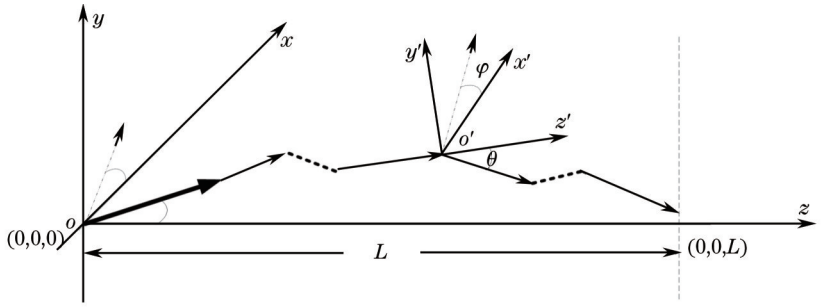

Fig.1 Schematic of the propagation procedure of a photon packet

2.2 Assumptions and simplifications

Similar to Ref.[23], computation complexity is decreased by making several assumptions when conducting Monte Carlo simulations. These assumptions are as follows: 1) water is homogeneous and stable, i.e., water parameters are unchanged throughout the communication procedure; 2) water volume is sufficiently large, and rendering boundary effects negligible; 3) the wavelength of photon packet remains unchanged after scattering; 4) the receiver is on the light-of-sight of the transmitted laser pulse. Obviously, the ULC system is a linear, shift- and time-invariant system.

2.3 Discussion on Monte Carlo method

Monte Carlo method is widely used for multi-scattering channel simulation, and its validation has been proven by many experiments[24-27]. The simulation procedure is simple and easy to understand.

However, Monte Carlo simulation still has some drawbacks. The simulation results are unusable when initial parameters change. The computation time of calculating the maximum communication distance of ULC is also difficult to predict. Generally, the detection threshold P_{D} is the decision criterion of the maximum communication distance. However, this parameter is not used for Monte Carlo simulation. Thus, the simulation procedure may be repeated many times until the maximum communication distance is derived. Obviously, that Monte Carlo method inefficiently calculates the maximum communication distance of ULC.

3 Semi-analytical method

To overcome the drawbacks of Monte Carlo method, we propose a semi-analytical method of calculating the maximum communication distance of a ULC system. For a given underwater optical channel, two reference distances can be obtained through simple mathematical calculation. For each reference distance, only one independent Monte Carlo simulation needs to be carried out. The maximum communication distance can be deduced based on the statistical results of the two simulations. Thus, we need to conduct Monte Carlo simulations

only twices when the semi-analytical method is used. When system parameters are changed, conducting simulation is not needed anymore. The semi-analytical method includes the following three steps.

3.1 Determining two reference distances

Underwater laser propagation in seawater can be defined by three propagation regimes[28]: directed/unscattered beam (for less than about 6 scattering lengths, scattering length L_{scat} is defined as $1/b$ [8]), multiple forward scattered beam ($6 < n_{scat} < 20$, $n_{scat} = L/L_{scat}$), and fully diffuse/multiple scattered beam ($n_{scat} > 20$). Supposing that the maximum communication distance belongs to fully diffuse/multiple scattered beam regime, we choose two transmission distances L_1 and L_2 as reference distances.

$$L_1 = 20L_{scat}, \tag{4}$$

$$L_2 = 40L_{scat}. \tag{5}$$

Thus, the reference distances L_1 and L_2 correspond with 20 and 40 scattering lengths, respectively. Choosing exactly 20 and 40 scattering lengths as the two reference distances is dispensible. However, to guarantee that reference distance is in fully diffuse/multiple scattered beam regime, reference distance should be not less than $20L_{scat}$.

3.2 Two simulation times

Apart from reference distances, initial parameters of photon packet, inherent optical properties (IOPs) of water, and receiving conditions should be also determined.

3.2.1 Initial parameters of photon packet

At the beginning of Monte Carlo simulation, initial energy, initial location, initial propagation direction and launch time of traced photon packets should be determined. Here, we set single pulse energy E_{T_MC} to 1 and the number of traced photon packets N to 10^8 considering both computation time and precision. Thus, the initial energy of a photon packet is $E_{P\_MC} = 10^{-8} E_{T\_MC}$. According to Ref. [8], the initial location of all photon packets is set to (0, 0, 0), the initial propagation direction is along the z axis, and the launch time is set to 0.

3.2.2 IOPs of water

In Monte Carlo simulation, the related IOPs of water include absorption coefficient a , scattering coefficient b , and asymmetry factor g . Given that these parameters are related to wavelength, laser wavelength should be chosen before simulations.

3.2.3 Receiving conditions

To guarantee the commonability of simulation results, instead of specifying receiver parameters, we adopt a plane with infinite size and full-view angle as receiving condition. States of the received photon packets should be recorded in a data file for subsequent use. For a receiver with specific aperture size and FOV, we need to extract only the corresponding photon packets from the data file. Thus, receiver parameters can be defined after simulations.

When the two simulation times are finished, the angular, temporal and spatial distributions on the receiving plane could be derived. Notably, the two simulation times are conducted based only on a given optical channel, and the system parameters have not yet been considered.

3.3 Equation derivation

The decision criterion of feasibility of a communication distance is whether the received laser power surpasses the detection threshold. The maximum communication distance corresponds with the distance where the received laser power equals the detection threshold. The received laser power relates only to the energy and full width at half maximum (FWHM) of temporal distribution of received laser pulse. To define the maximum communication distance of a specific ULC system, we need to study the influences of system parameters on the energy and width of received laser pulse.

3.3.1 Influence of transmitter

The parameters of a transmitter include single pulse energy, transmission efficiency, initial beam radius, far-field

divergence angle and initial pulse width. ULC is a linear and shift-invariant system; thus, single pulse energy and transmission efficiency influence only the received energy. Moreover, the spatial distribution of laser beam on the receiving plane is a two-dimensional convolution of its initial spatial distribution and the spatial impulse response of the channel[29]. The spatial impulse response refers to the spatial distribution on receiving plane when all photon packets are launched from (0, 0, 0). Generally, initial laser beam size is much smaller than receiver radius, so initial laser beam can be treated as a spot. Thus, the influence of initial beam radius is negligible. In practical applications, a collimated laser beam is used to increase the maximum communication distance as much as possible, so far-field divergence angle is controlled to less than several milliradians. Seawater is a multiple-scattering medium for a laser. After multiple scattering ($n_{\mathrm{scat}}>20$), initial divergence angle within several milliradians is also negligible. Furthermore, the temporal distribution of a received laser pulse is the convolution of its initial temporal distribution and the impulse response of system[30]. To simplify calculation, Gaussian distribution is adopted to approximate the shape of transmitted laser and impulse response[31]. The convolution of two Gaussian distributions is also Gaussian distribution, and the FWHM of Gaussian distribution τ_{Gauss} equals to $2\sqrt{2\ln 2}\,\sigma_{\mathrm{Gauss}}$, where σ_{Gauss} is the variance of Gaussian distribution. For a transmitted δ pulse, the simulated FWHM of received pulse is denoted by τ_{L_MC} (L denotes transmission distance and MC denotes Monte Carlo simulation). If the initial laser pulse width is τ_0, the FWHM of received pulse is

$$\tau_L=\sqrt{\tau_{L\_\mathrm{MC}}^2+\tau_0^{\,2}}\,. \tag{6}$$

In summary, for the transmitter of a ULC system, we need to consider only the influence of single pulse energy, transmission efficiency and initial width.

3.3.2 Influence of receiver

Parameters of receiver include receiving efficiency, aperture radius and FOV. Similar to transmission efficiency, receiving efficiency influences only received energy. For a certain aperture radius and FOV, photon packets that satisfy the receiving condition can be conveniently extracted from the data file. The data file is generated during the two simulation times, in which the states of all photon packets are stored on receiving plane. By summing up the energy of these photon packets according to their arrival time, we obtain the temporal distribution of received pulse. In the case of $L=L_1$ and $L=L_2$, received energy is denoted by $E_{L_1\_\mathrm{MC}}$ and $E_{L_2\_\mathrm{MC}}$, and the pulse width of received laser is denoted by $\tau_{L_1\_\mathrm{MC}}$ and $\tau_{L_2\_\mathrm{MC}}$, respectively.

Here, considering a practical ULC system, we obtain the received energy E_{L_1} and E_{L_2}, as well as the pulse width τ_{L_1} and τ_{L_2}.

$$E_{L_1}=E_{\mathrm{T}}\frac{E_{L_1\_\mathrm{MC}}}{E_{\mathrm{T\_MC}}}\eta_{\mathrm{S}}\eta_{\mathrm{R}}\,, \tag{7}$$

$$E_{L_2}=E_{\mathrm{T}}\frac{E_{L_2\_\mathrm{MC}}}{E_{\mathrm{T\_MC}}}\eta_{\mathrm{S}}\eta_{\mathrm{R}}\,, \tag{8}$$

$$\tau_{L_1}=\sqrt{\tau_{L_1\_\mathrm{MC}}^2+\tau_0^2}\,, \tag{9}$$

$$\tau_{L_2}=\sqrt{\tau_{L_2\_\mathrm{MC}}^2+\tau_0^2}\,, \tag{10}$$

where E_{T} is the single pulse energy of the practical ULC system, and η_{S} and η_{R} are transmission and receiving efficiencies, respectively.

Both received energy and received pulse width change with transmission distance. The received energy decays exponentially with the increase of transmission distance[23]. Energy decay coefficient can be defined by

$$k_{\mathrm{E}}=-\frac{\ln(E_{L_2}/E_{L_1})}{L_2-L_1}\,. \tag{11}$$

Received pulse width roughly increases linearly with the increase of transmission distance[32-33]. Scale factor can

be defined by

$$k_{\mathrm{T}}=\frac{\tau_{L_2}-\tau_{L_1}}{L_2-L_1}. \tag{12}$$

The maximum communication distance of ULC system is defined as transmission distance where received pulse power equals detection threshold, i.e.,

$$P_{\mathrm{D}}=\frac{E_{L_1}\exp[-k_{\mathrm{E}}(L_{\max}-L_1)]}{\tau_{L_1}+k_{\mathrm{T}}(L_{\max}-L_1)}, \tag{13}$$

where P_{D} is detection threshold, and $L_{\max}$ is the maximum communication distance.

Finally, the semi-analytical equation is obtained. The equation is described as semi-analytical rather than analytical because some parameters used in the equation need to be obtained from simulation results. Although Eq. (13) is an implicit equation for $L_{\max}$, obtaining $L_{\max}$ through calculation, especially through programming, is convenient.

We now discuss the application scope of Eq. (13). The beam spot should be limited to within several millimeters, and the far-field divergence angle should be limited to within several nanoseconds. If these conditions are not satisfied, calculation error may be obvious. In section 3.1, we suppose that the maximum communication distance is in fully diffuse/multiple scattered beam regime. If the final calculated maximum communication distance $L_{\max}<20L_{\mathrm{scat}}$ (caused by too low single pulse energy or too high detection threshold), calculation results would not be credible.

4　Experimental validation

To validate the calculation method proposed in this paper, we compare the simulation results with experimental ones. Fig.2 shows the schematic of field experiment. The transmitter is sealed in a cylindrical water-tight container and placed on the bottom of water tank. The laser pulse is launched through the output window of container. The receiver is also sealed in a cylindrical water-tight container and submerged in water. After photoelectric conversion and a series of processing, the signal is sent to a personal computer for monitoring and display.

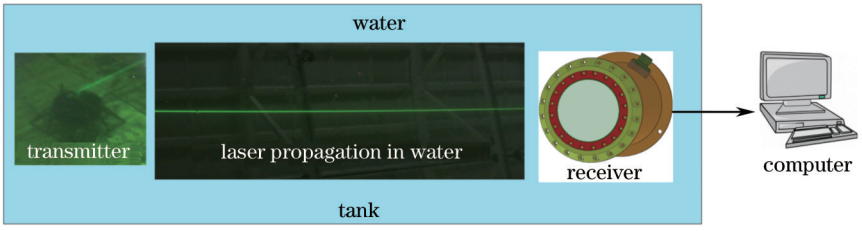

Fig.2　Schematic of field experimental setup

System parameters and experimental results are listed in Table 1. The experiment is conducted in a long tank. In the experiment, the detection threshold is set to 10 nW to guarantee a bit error rate of less than 10^{-5}.

Table 1　System parameter

Parameter	Value
Wavelength /nm	532
Single pulse energy E_{T} /mJ	4
Initial spot radius /mm	1
Far field divergence angle /mrad	2
Initial pulse width τ_0 /ns	10
Send efficiency η_{S}	0.8
Receiving effiviency η_{R}	0.4
Detection threshold P_{D} /nW	10
Aperture radius /mm	50
Field of view /(°)	2

As an example, we calculate the maximum communication distance according to the procedure shown in section 3.

Step 1. The two reference distances are calculated. The experiment is conducted in case-III water, whose attenuation coefficient is 0.51 m^{-1} for 532 nm wavelength. Referring to the albedo 0.81 of case-III water[28], absorption and scattering coefficients (a,b) are $(0.096,0.414)$. Thus, the two reference distances (L_1,L_2) are set to (48.3 m,96.6 m).

Step 2. Monte Carlo simulation is conducted. In simulations, g is set to 0.924[3]. After simulation, the angular, temporal and spatial distributions on receiving plane are obtained. The states of photons arriving on the receiving plane are recorded in a data file for subsequent use. FWHM and spot radius (defined as the smallest radius that encompasses 87.5% of the total energy) are also shown in corresponding subfigures. In these temporal distribution subfigures, common delay time (the time which a photon takes to propagate directly from transmitter to receiver without collision) is subtracted. The laser is observed to be diffuse. FWHM is about tens of nanoseconds, and spot radius is about tens of meters. With increased transmission distance, random fluctuations become obvious.

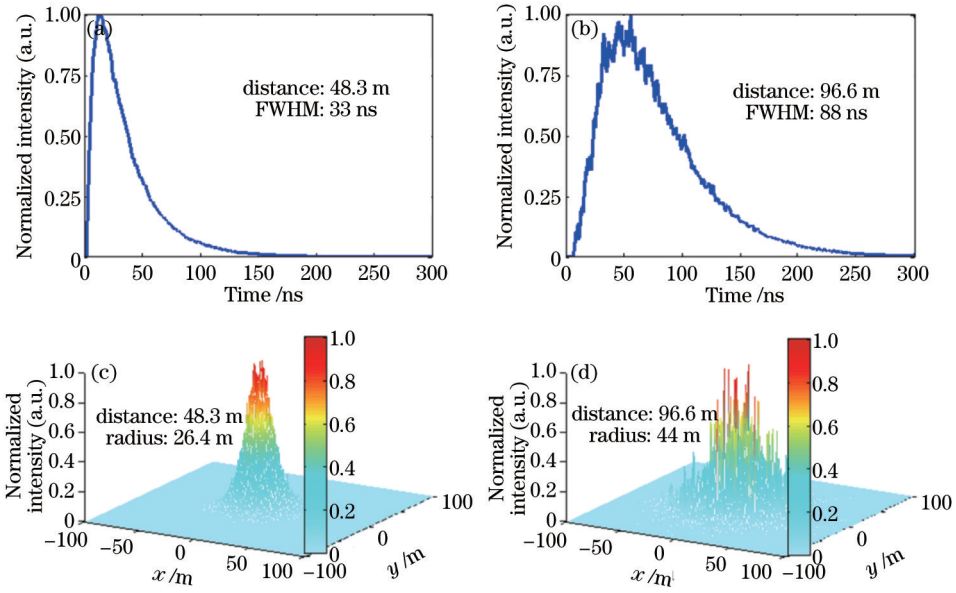

Fig.3 Temporal and spatial distributions on receiving plane. (a) Temporal distribution when $L=48.3$ m; (b) temporal distribution when $L=96.6$ m; (c) spatial distribution when $L=48.3$ m; (d) spatial distribution when $L=96.6$ m

Step 3. The maximum communication distances are calculated. Firstly, according to the aperture radius and FOV of the receiver, we extract the photons that satisfy the receiving condition from the data file recorded in step 2. Through accumulation, we obtain the energy and pulse widths of received lasers. The energy decay coefficient k_E and pulse width growth factor k_T could be derived from Eq. (11) and Eq. (12). Finally, approximately 83.6 m of the maximum communication distance is derived from Eq. (13). Simulation parameters and statistical results are listed in Table 2. For convenience of comparison, we list the tested maximum communication distance in Table 2. The difference between calculated and tested maximum communication distance is 2.6%. Given that the two results coincide with each other, the validity of the proposed semi-analytical method can be proven.

The difference between the calculated and tested results may be brought by the following: 1) the IOP parameters used in simulations being not the actual IOP parameters of the water in tank, 2) the Gaussion pulse approximation in simulation. In fact, the pulse shape is closer to γ function[34].

Table 2 Simulation parameters and statistical results

Classification	Parameter	Value
Initial parameter	Absorption coefficient a	0.096
	Scattering coefficient b	0.414
	Attenuation coefficient c	0.51
	Asymmetry factor g	0.924
Intermediate calculation variable	First reference distance L_1 /m	48.3
	Second reference distance L_2 /m	96.6
	Energy in the first reference distance $E_{L_{1\_MC}}/E_{T\_MC}$ /10^{-11}	5.6
	Energy in the second reference distance $E_{L_{2\_MC}}/E_{T\_MC}$ /10^{-12}	8.0
	Pulse width in the first reference distance $\tau_{L_{1\_MC}}$ /ns	2
	Pulse width in the second reference distance $\tau_{L_{2\_MC}}$ /ns	6
	Energy decay coefficient k_E /(m^{-1})	0.183
	Pulse width growth factor k_T /(ns/m)	0.03
Final result	Simulated maximum communication distance $L_{max,simulated}$ /m	83.6
	Tested maximum communication distance $L_{max,tested}$ /m	85.8
	Difference /%	2.6

5 Conclusion

An original semi-analytical method is proposed to calculate the maximum communication distance of ULC system. The calculation equation is also derived. Compared with conventional Monte Carlo method, the semi-analytical method is more rapid and predictable, which makes it especially useful in rapidly estimating the maximum communication distances under changed system conditions. Our experimental results prove the validity of the semi-analytical method.

References

1 M Lanzagorta. Underwater Communications[M]. Morgan & Claypool, 2013.

2 S Arnon. Optical wireless communication through random media[C]. SPIE, 2011, 7924: 7924D.

3 C Gabriel, M A Khalighi, S Bourennane, *et al*.. Monte-Carlo-based channel characterization for underwater optical communication systems[J]. Journal of Optical Communications and Networking, 2013, 5(1): 1-12.

4 N Farr, A D Chave, L Freitag, *et al*.. Optical modem technology for seafloor observatories[C]. Oceans 2006, 2006: 928 - 934.

5 C Detweiller, I Vasilescu, D Rus. An underwater sensor network with dual connunications, sensing, and mobility[C]. Oceans 2007, 2007: 1-6.

6 M Doniec, I Vasilescu, M Chitre, *et al*.. Aqua Optical: A lightweight device for high-rate long-range underwater point-to-point communication[C]. Oceans 2009, 2009: 1- 6.

7 W Wei, X H Zhang, J H Rao, *et al*.. Time domain dispersion of underwater optical wireless communication[J]. Chin Opt Lett, 2011, 9 (3): 030101.

8 R M Lerner, J D Summers. Monte Carlo description of time- and space-resolved multiple forward scatter in natural water[J]. Appl Opt, 1982, 21(5): 861-869.

9 L Mullen, D Alley, B Cochenour. Investigation of the effect of scattering agent and scattering albedo on modulated light propagation in water[J]. Appl Opt, 2011, 50(10): 1396-1404.

10 F Hanson, S Radic. High bandwidth underwater optical communication[J]. Appl Opt, 2008, 47(2): 277-283.

11 Wang Wei, Chu Jinkui, Cui Yan, *et al*.. Modeling of atmospheric polarization pattern based on vector radiative transfer[J]. Chinese J Lasers, 2013, 40(5): 0513001.

王　威, 褚金奎, 崔　岩, 等. 基于矢量辐射传输的大气偏振建模[J]. 中国激光, 2013, 40(5): 0513001.

12 Chen Feinan, Chen Yanru, Zhao Qi, *et al*.. Change of propagation quality factor of partically coherence Hermite-Gaussian beams travelling through oceanic turbulence[J]. Chinese J Lasers, 2013, 40(4): 0413002.

陈斐楠, 陈延如, 赵　琦, 等. 部分相干厄米高斯光束在海洋湍流中光束传输质量的变化[J]. 中国激光, 2013, 40(4): 0413002.

13 E Q Zhan, H Y Wang. Research on spatial spreading effect of blue-green laser propagation through seawater and atmosphere[C]. E-Business and Information System Security, 2009: 1-4.

14 C Gabriel, M Khalighi, S Bourennane, *et al*.. Channel modeling for underwater optical communication[C]. 2nd IEEE Workshop on Optical Wireless Communications, 2011: 833-837.

15 K Turpin, J G Walker, P C Y Chang, *et al*.. The influence of particle size in active polarization imaging in scattering media[J]. Opt Commun, 1999, 168: 325-335.

16 Liu Jintao, Chen Weibiao. Feasibility study of laser communications from satellite to submerged platform[J]. Acta Optica Sinica, 2006, 26(10): 1441-1446.

刘金涛, 陈卫标. 星载激光对水下目标通信可行性研究[J]. 光学学报, 2006, 26(10): 1441-1446.

17 Liang Bo, Zhu Hai, Chen Weibiao. Simulation of laser communication channel from atmosphere to ocean[J]. Acta Optica Sinica, 2007, 27(7): 1166-1172.

梁　波, 朱　海, 陈卫标. 大气到海洋激光通信信道仿真[J]. 光学学报, 2007, 27(7): 1166-1172.

18 Wang Ziqian, Zhang Xudong, Jin Haihong, *et al*.. All sky turbid atmosphere polarizacation pattern modeling based on Monte Carlo method[J]. Chinese J Lasers, 2014, 41(10):1013001.

王子谦, 张旭东, 金海红, 等. 基于Monte Carlo方法的混浊大气偏振模式全天域建模[J]. 中国激光, 2014, 41(10): 1013001.

19 Liu Qi, Chu Jinkui, Wang Jing, *et al*.. Research and simulation analysis of atmosphere polarization properties under water cloud condition[J]. Acta Optica Sinica, 2014, 34(3): 0301004.

刘　琦, 褚金奎, 王　兢, 等. 水云条件下大气偏振特性研究及其模拟分析[J]. 光学学报, 2014, 34(3): 0301004.

20 Wei Anhai, Zhao Wei, Han Biao, *et al*.. Simulative study of optical pulse propagation in water based on Fournier-Forand and Henyey-Greenstein volume scattering functions[J]. Acta Optica Sinica, 2013, 33(6): 0601003.

魏安海, 赵　卫, 韩　彪, 等. 基于Fournier-Forand和Henyey-Greenstein体积散射函数的水中光脉冲传输仿真分析[J]. 光学学报, 2013, 33(6): 0601003.

21 J Li, Y Ma, Q Q Zhou, *et al*.. Channel capacity study of underwater wireless optical communications links based on Monte Carlo simulation[J]. Journal of Optics, 2012, 14(1): 015403.

22 Z Hajjarian, M Kavehrad, J Fadlullah. Analysis of wireless optical communications feasibility in presence of clouds using Markov chains[J]. IEEE J Sel Area Comm, 2009, 27(9): 1526-1534.

23 Jr Cox W C. Simulation, Modeling, and Design of Underwater Optical Communication Systems[D]. Raleigh: North Carolina State University, 2012: 161-162.

24 E A Bucher. Computer simulation of light pulse propagation for communication through thick clouds[J]. Appl Opt, 1973, 12(10): 2391-2400.

25 E A Bucher, R M Lerner. Experiments on light pulse communication and propagation through atmospheric clouds[J]. Appl Opt, 1973, 12(10): 2401-2414.

26 G C Mooradian, M Geller, L B Stotts, *et al*.. Blue-green pulsed propagation through fog[J]. Appl Opt, 1979, 18(4): 429-441.

27 R A Elliott. Multiple scattering of optical pulses in scale model clouds[J]. Appl Opt, 1983, 22(17): 2670-2681.

28 G Mooradian. Undersea laser communications is a "game-changer" for the US navy, so how do we make the promise a reality?[C]. Photonics Society Summer Topical Meeting Series, 2012: 71-72.

29 A V Oppenheim, R W Schafer. Digital Signal Processing[M]. Upper Saddle River: Prectice Hall Inc, 1975.

30 S Jaruwatanadilok. Underwater wireless optical communication channel modeling and performance evaluation using vector radiative transfer theory[J]. IEEE J Sel Area Commum, 2008, 26(9): 1620-1627.

31 C Y Young, L C Andrews, A Ishimaru. Time-of-arrival fluctuations of a space-time Gaussian pulse in weak optical turbulence: An analytic solution[J]. Appl Opt, 1998, 37(33): 7655-7660.

32 Zhou Yamin, Liu Qizhong, Zhang Xiaohui, *et al*.. An efficient method for simulating time-domain broadening of laser pulse propagating underwater[J]. Chinese J Lasers, 2009, 36(1): 143-147.

周亚民, 刘启忠, 张晓晖, 等. 一种激光脉冲水下传输时域展宽模拟计算方法[J]. 中国激光, 2009, 36(1): 143-147.

33 P Lacovara. High-bandwidth underwater communications[J]. Marine Technology Society Journal, 2008, 42(1): 93-102.

34 G C Mooradian, M Geller. Temporal and angular spreading of blue-green pulses in clouds[J]. Appl Opt, 1982, 20(9): 1572-1577.

栏目编辑：王晓琰